318–325 Nucleic Acids Research, 1997, Vol. 25, No. 2

The SRP9/14 subunit of the human signal recognition particle binds to a variety of Alu-like RNAs and with higher affinity than its mouse homolog

Fabrice Bovia, Nicole Wolff, Stephan Ryser and Katharina Strub*

Département de Biologie Cellulaire, Université de Genève, Sciences III, CH-1211 Geneva 4, Switzerland

Received October 8, 1996; Revised and Accepted November 21, 1996

ABSTRACT

The heterodimeric subunit, SRP9/14, of the signal recognition particle (SRP) has previously been found to bind to scAlu and scB1 RNAs *in vitro* and to exist in large excess over SRP in anthropoid cells. Here we show that human and mouse SRP9/14 bind with high affinities to other Alu-like RNAs of different evolutionary ages including the neuron-specific BC200 RNA. The relative dissociation constants of the different RNA–protein complexes are inversely proportional to the evolutionary distance between the Alu RNA species and 7SL RNA. In addition, the human SRP9/14 binds with higher affinity than mouse SRP9/14 to all RNAs analyzed and this difference is not explained by the additional C-terminal domain present in the anthropoid SRP14. The conservation of high affinity interactions between SRP9/14 and Alu-like RNAs strongly indicates that these Alu-like RNPs exist *in vivo* and that they have cellular functions. The observation that human SRP9/14 binds better than its mouse counterpart to distantly related Alu RNAs, such as recently transposed elements, suggests that the anthropoid-specific excess of SRP9/14 may have a role in controlling Alu amplification rather than in compensating a defect in SRP assembly and functions.

INTRODUCTION

The signal recognition particle (SRP), a cytoplasmic ribonucleoprotein particle, mediates co-translational translocation of proteins into the endoplasmic reticulum (ER) in eukaryotic cells (1,2). SRP specifically recognizes the signal sequences of nascent chains and subsequently targets the nascent chain–ribosome complex to the membrane of the ER. During the targeting process, SRP effects a delay or an arrest in the elongation of the nascent chain thereby ensuring a cotranslational mode of protein translocation (3). The elongation arrest activity of SRP is dependent on its signal recognition function, which resides in the 54 kDa subunit (SRP54), and on the components in the Alu-domain of SRP (3,4). The Alu-domain comprises the sequences at the 5′ and 3′ ends of 7SL RNA (SRP RNA) that are homologous to the Alu family of repetitive sequences and two polypeptides SRP9 and SRP14. How these components interact with the ribosome to effect elongation arrest remains to be elucidated.

SRP9 and SRP14 proteins form a stable heterodimer (SRP9/14) and it is exclusively the heterodimer that binds with high specificity to 7SL RNA (5). The SRP14 proteins in higher primates (anthropoids) are larger than other mammalian SRP14 proteins (6–8). The observed size variation is due to the translation of a GCA trinucleotide repeat at the 3′ end of the coding region of SRP14. The additional C-terminal domain in the protein is composed of alanines, few threonines and prolines and varies in size from 26 to 54 amino acids depending on the anthropoid species. The expansion of the GCA trinucleotide repeat occurred upon divergence of the prosimians and the anthropoids, concomitantly with the duplication of the SRP14 gene. During anthropoid evolution, the repetitive sequence was shortened again and the human protein has the smallest, 26 amino acids long, additional C-terminal domain. Furthermore, SRP14 and SRP9 proteins in anthropoids were found to accumulate in a 20-fold excess over SRP, probably due to an increased synthesis rate of both proteins (6–8).

The SRP subunit SRP9/14 has recently been shown to bind to small cytoplasmic Alu RNAs (scAlu RNAs) *in vitro* and *in vivo* (6,7,9) suggesting the existence of a novel class of scRNPs that contain RNA and protein subunits related to SRP (for review see ref. 10). The RNA moieties of these novel scRNPs are matured transcripts derived from the Alu family of repetitive sequences in the primate genome (11,12). The very abundant (~1 million copies in the human genome) and highly dispersed Alu sequences are phylogenetically derived by retroposition from the 5′ and 3′ terminal sequences of the 7SL gene (for review on Alu sequences see refs 13 and 14). The amplification rate of Alu elements has been much higher in anthropoids than in prosimian and rodents (15–18). The oldest Alu elements identified so far, the fossil Alu monomers (FAM), contain one copy of the Alu sequences of the 7SL RNA gene. The FAM elements diverged into the families of the free left (FLAM) and the free right (FRAM) Alu monomers (19–21). The modern Alu repetitive element is composed of a right and a left Alu monomer which are separated and followed by A-rich tracts (14). The dimeric Alu repeats were classified into subfamilies of distinctive evolutionary ages (22). The Alu RNAs that were found to accumulate in the cytoplasm of primate cells include dimeric Alu and scAlu RNAs that are transcribed from various loci representing predominantly younger Alu subfa-

*To whom correspondence should be addressed. Tel: +41 22 702 6724; Fax: +41 22 781 1747; Email: strub@cellbio.unige.ch

milies. The dimeric and scAlu RNAs accumulate at ~10^3 and 10^4 copies per cell, respectively, and exist as RNPs (9,12,23). The BC200 RNA, another Alu-like RNA in primates, is expressed from a single gene that is highly homologous to the FLAM sequences and more closely related to the 7SL RNA gene than to dimeric Alu elements. In addition to the Alu sequences at its 5′ end, BC200 RNA contains a central adenine-rich region and 43 unique terminal nucleotides. The BC200 RNA is expressed in a subset of neurons in primates and localizes specifically to the somato-dentritic region (24,25).

The rodent genome contains B1 repetitive elements, which are monomeric (26). A subset of B1 elements are transcriptionally active and expressed as matured small cytoplasmic B1 RNAs (scB1 RNA) (27,28). The scB1 RNAs were also found to bind to human SRP9/14 *in vitro* (9,29). The 4.5S RNA genes represent another family of Alu-related sequences in rodents that lacks 3′ terminal sequences as compared with B1 elements (30). The 4.5S RNA lack the typical cruciform structure at the 5′ end of 7SL RNA (28,31). The putative functions of Alu-related scRNPs in rodents and primates remains to be elucidated.

The addition of the C-terminal tail in SRP14 and the overexpression of SRP9 and SRP14 proteins as well as the major amplification of Alu sequences occurred during the same evolutionary period suggesting a relationship between the events (8). We wanted to examine whether Alu-like RNAs other than scAlu and scB1 RNAs can bind to SRP9/14. Furthermore, we wanted to compare the relative affinities of human and mouse SRP9/14 for various Alu-like RNAs. Our results demonstrate that both heterodimers bind to a large variety of Alu-like RNAs, and that the human SRP9/14 heterodimer binds significantly better than murine SRP9/14 to all of them, including the murine scB1 RNA. The difference between the two proteins is not due to the additional C-terminal domain, but resides within the conserved portion of the two proteins. The affinities of both proteins for the RNAs decrease with increasing evolutionary distance between the Alu RNA and 7SL RNA, however, human SRP9/14 preserved a high affinity for even very distantly related Alu RNAs, such as recently transposed Alu elements, indicating a possible function for these complexes in Alu amplification.

MATERIALS AND METHODS

Purification of mSRP9/14, hSRP9/14 and hSRP9/14ΔR

The coding regions of human and murine SRP14 and SRP9 cDNAs (6,32,33), (the human SRP9 cDNA was a kind gift of H. Leffers) were inserted into the *Nde*I and *Bam*HI sites of the pET expression vectors (34). The murine SRP9 and SRP14 coding regions were inserted into two independent T7 transcription units in tandem on the same plasmid (pET9a). To this end, the SRP9 and SRP14 coding regions were first inserted into the *Nde*I and *Bam*HI sites of pET3a and 9a, respectively (pE9C and pE14Kan). The SRP9 coding region and the adjacent T7 promotor and terminator sequences were then amplified with the polymerase chain reaction (PCR) from the plasmid pE9C using an oligonucleotide that was complementary to the sequences comprising the *Bgl*II site of pET3a and an oligonucleotide that introduced a *Bcl*I site at the *Eco*RV site in pET3a. The amplified DNA was cut with the restriction enzymes *Bcl*I and *Bgl*II and the fragment inserted into the *Bgl*II site of the pE14Kan plasmid resulting in plasmid pE9-14dim. In pE9-14dim, the transcription unit containing SRP9 sequences precedes the one containing the SRP14 sequences. Because of the instability of murine SRP14 in bacteria, SRP9 accumulates in excess over SRP14 in bacteria expressing both proteins. To express the truncated human SRP14 protein (hSRP14ΔR), the codon of alanine 108 in the human SRP14 cDNA was changed to a stop codon by PCR. The coding regions of all expression plasmids were sequenced. Bacteria BL21(DE3) transformed with the different plasmids were grown in a 1 l culture and protein synthesis induced with 0.8 mM isopropyl-β-D-thiogalactopyranoside for 3 h. Clarified cell lysate were obtained as described (35). Lysates containing SRP9 and SRP14 were combined at a ratio of 2:1. After 30 min at 4°C, both reconstituted dimers were purified on 15 ml heparin and CM columns (Bio-Rad). The concentrations of the purified proteins were quantified by measuring the optical density at 280 nm. The specific absorption coefficient was calculated based on the absorptions of tyrosine and tryptophane which are 1.2 and 5.6 A_{280}/mM respectively.

Plasmids expressing various Alu-like RNAs

The constructs p7S1-A, p7Salu, p7Sswt and pSscAlu were described previously (6,35,36). pSscAlu was renamed in this paper to pSscAlu/LDL. Generally, the Alu sequences were amplified from various cDNAs with the PCR using 5′ primers, which add the T7 RNA polymerase promotor at the correct position at the 5′ end, and 3′ primers, which introduce a restriction site at the 3′ end of the RNA sequences. The scAlu/α-feto RNA and the dimeric Alu RNA sequences were amplified from the human α-fetoprotein gene (nt 5059–5176 and nt 5059–5345, respectively) (37). BC200 RNA sequences were amplified from the BC200 RNA gene (24).The scB1 sequences were amplified from the pscB1-10 cDNA clone (28). The 4.5S RNA sequences were amplified from the genomic clone (pSP64-4.5S) of 4.5S RNA (38). The right Alu monomer sequences were amplified from C33 antigen cDNA (nt 1463–1617) (39). The resulting plasmids, pPscAlu/α-feto, pPAluRNA, pPBC200, pSscB1, pS4.5S and pSright were linearized with *Spe*I, *Ssp*I, *Dra*I, *Xho*I, *Dra*I and *Nde*I, respectively, for *in vitro* transcription. The plasmids expressing U2, U4 and BC1 RNA were kind gifts from Angela Krämer, Patrizia Fabrizio and Dieter Zopf, respectively.

RNA binding experiment of Alu-like RNAs to SRP9/14

hSRP14 and mSRP14 were synthesized in wheat germ extract as previously described (6,35). The ^{35}S-labeled proteins were bound in the presence and in the absence of recombinant mSRP9 (1 pmol/binding reaction) (3) to 1 pmol biotinylated RNA in 50 mM HEPES–KOH pH 7.5, 350 mM potassium acetate, 3.5 mM magnesium acetate and 0.01% Nikkol. The bound and free proteins were separated using streptavidin beads as described in (35).

Large scale *in vitro* transcription

Large scale transcriptions were done in 1 ml of 40 mM Tris–HCl pH 8.1, 1 mM spermidine, 1 mg/ml bovine serum albumin (BSA, Sigma), 0.01% Triton X-100, 5 mM DTT, 25 mM $MgCl_2$, 1 mM each NTP, 39 U/ml RNase inhibitor (Promega), 50 ng/µl linearized DNA, 10 U/µl T7 RNA polymerase. After 2 h at 37°C, the RNA was purified on a preparative 7.5 M urea/8% PAGE. The RNA was visualized by UV shadowing and the main band was excised and eluted from the gel with 5 ml 0.3 M sodium acetate for 4 h at 4°C.

After ethanol precipitation, the RNA was dissolved in 10 mM HEPES–KOH pH 7.0 and stored at 4°C. The quality of the different RNAs was controlled by analytical 7.5 M urea/8% PAGE.

Labeling of 7S-Alu RNA

Labeling of 7S-Alu RNA with [α-^{32}P]UTP was carried out in 10 µl transcription reactions containing 1 mM each ATP, CTP, GTP, 20 µCi [α-^{32}P]UTP (800 Ci/mmol) (Amersham), 0.2 U/µl RNase inhibitor, 50 ng/µl linearized DNA and 10 U/µl T7 RNA polymerase. After 2 h at 37°C, the labeled RNA was purified by 7.5 M urea/8% PAGE. The concentration of the RNA was calculated from the specific activity of the [α-^{32}P]UTP and from the number of UTPs present in the transcript. A 50-fold excess in weight of poly(rG) (Boehringer) was added as a non-specific competitor to the eluted RNA before ethanol precipitation.

Complex formation and nitrocellulose filter binding assays

RNA and protein were combined in a total volume of 10 µl 50 mM HEPES–KOH pH 7.5, 250 mM potassium acetate, 5 mM magnesium acetate, 0.01% Nikkol, 1 mM DTT, 10 µg/ml bovine serum albumin and 39 U/ml RNase inhibitor (binding buffer). Samples were incubated for 10 min at 0°C and 10 min at 37°C and were then transferred on ice. Samples were filtered without dilution through nitrocellulose at 4°C and were washed once with 200 µl 50 mM HEPES–KOH pH 7.5, 250 mM potassium acetate, 5 mM magnesium acetate, 1 mM DTT and once with 100 µl of the same buffer but containing 100 mM potassium acetate. Additional washes had no effect on the amount of RNA retained on the filter indicating that the complex was stable. To determine the amount of radiolabeled RNA used in the experiments (R_o), we spotted several dilutions of the RNA onto the filter. Membranes were subsequently dried, cut and the amount of labeled RNA retained on the nitrocellulose filter was determined by liquid scintillation counting.

Simple binding experiments

^{32}P-labeled 7S-Alu RNA was diluted in binding buffer, split into eight aliquots (8 µl/sample) and combined with 2 µl aliquots of the different heterodimeric proteins in binding buffer. The final concentration of labeled RNA was constant at 0.04 nM whereas the concentrations of the proteins varied as indicated. A simple bimolecular binding reaction served as the bases of our calculations: R + P↔RP where R and P represent the RNA and the protein, respectively. The dissociation constant is defined by $K_d = [R] \times [P]/[RP]$. Under the experimental conditions used, [RP] is small compared with P_0 and the formula can be modified into the Scatchard equation (40):

$$\upsilon/P_0 = -1/K_d \times \upsilon + 1/K_d \qquad \mathbf{1}$$

P_0 represents the protein concentration used in the experiment and υ is the fraction of the RNA in the complex at a given protein concentration. The retention efficiencies of the RNA samples were constant at saturating protein concentrations for the same RNA–protein complexes. It was at 65% for both human heterodimers and at 25% for the murine heterodimer. Low retention efficiencies have previously been observed for other RNA–protein complexes (41–43). The fraction of RNA bound at saturating protein concentrations was normalized to 1. The activities of the proteins were determined by mixing a constant high concentration of 7S-Alu RNA (containing a trace of ^{32}P-labeled 7S-Alu RNA) in binding buffer (8 µl/sample) with various amount of proteins (2 µl/sample). The final concentration of cold RNA was 25 nM.

Direct competition experiments

A mix containing a constant amount of cold 7S-Alu RNA and ^{32}P-labeled 7S-Alu RNA as a tracer was split in different aliquots (6 µl/sample) containing different amounts of cold competitor RNA (2 µl/sample). Based on the results of the simple binding experiments, the concentrations of 7S-Alu RNA and of the protein were chosen to ensure 98% binding of the protein. Samples were mixed and incubated with a constant amount of proteins (2 µl/sample). The final concentration of unlabeled 7S-Alu RNA and protein was 30 and 25 nM, respectively.

$$\frac{K_{d7S\text{–}Alu}}{K_{dcomp.}} = \frac{R_{07S\text{–}Alu}}{R_{0comp.}} \times \frac{[R_{comP}]}{[R_{07S\text{–}Alu}P]} \qquad \mathbf{2}$$

Taking into consideration that, $[R_{comp}P] = (\upsilon_0 - \upsilon) \times R_{07S\text{-}Alu}$; $[R_{7S\text{-}Alu}P] = \upsilon \times R_{07S\text{-}Alu}$ and $R_{comp} = R_{0comp} - [(\upsilon_0 - \upsilon) \times R_{07S\text{-}Alu}]$, this equation can be transformed into equation **3** where the slope represents $K_{dcomp}/K_{d7S\text{-}Alu}$.

$$\frac{R_{0comp}}{R_{07S-Alu}(\upsilon_o - \upsilon)} - 1 = \frac{K_{dcomp}}{K_{d7S-Alu}} \times [\frac{1}{\upsilon} - 1] \qquad \mathbf{3}$$

The left side of the equation is denominated by F in the graphical representation. $R_{07S\text{-}Alu}$ and R_{0comp} are the input concentrations of 7S-Alu and competitor RNAs, respectively. The fraction of complexed 7S-Alu RNA at different competitor concentrations is represented by υ. The fraction of complexed 7S-Alu RNA in the absence of competitor RNA is designated υ_0. The retention efficiencies of the labeled and unlabeled RNAs were considered to be the same in these experiments.

RESULTS

SRP9/14 proteins bind to a large variety of small cytoplasmic RNAs phylogenetically related to the Alu sequences of 7SL RNA

Human SRP9/14 was found to bind scAlu and scB1 RNAs *in vitro*. We wanted to examine more generally which of the RNAs that are phylogenetically derived from the terminal portions of 7SL RNA can bind to the SRP subunit SRP9/14. We engineered a series of plasmids for the synthesis of the different Alu-like RNAs with T7 RNA polymerase. A complete dimeric Alu sequence with a short poly A tail was obtained from the human α-fetoprotein gene. Left Alu monomers, which are descendants of the ancestral FLAM elements, were obtained from the human α-fetoprotein gene (scAlu/α-feto) and from the human LDL receptor cDNA (scAlu/LDL). An Alu sequence representing the right monomer (right) of a dimeric Alu element was obtained from the C33-antigen cDNA. The right monomers are derived from the ancestral FRAM elements. We also prepared expression plasmids for murine RNAs that are phylogenetically derived from 7SL RNA such as scB1 and 4.5S RNAs. Two other constructs were made to express the neuron-specific human BC200 and rat BC1 RNAs. BC200 and BC1 RNAs are thought to be functional homologues, based on their same specific expression patterns and on their same subcellular location. However, BC1 RNA is phylogenetically derived from the $tRNA^{Ala}$ gene (44). The dimeric Alu sequences were classified into subfamilies of

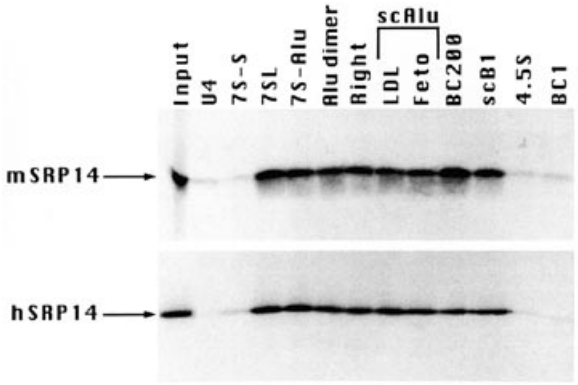

Figure 1. RNA-binding capacities of different Alu-like RNAs. *In vitro* synthesized ^{35}S-labeled human and murine SRP14 combined with recombinant murine SRP9 were bound to different biotinylated RNAs as indicated on top of each lane. The RNA-bound proteins were displayed by SDS–PAGE followed by autoradiography. Input: 1/3 of the amount of ^{35}S-labeled human and murine SRP14 proteins used in the experiments. The different RNAs are described in the text. No SRP14-binding to the RNAs was observed in the absence of SRP9 (not shown).

different evolutionary ages based upon diagnostic mutations shared by subfamily members (18,45). The scAlu/α-feto and scAlu/LDL represent Alu sequences of the old and fixed AluS and the young and mobile AluYb8 families, respectively. The right monomer of the dimeric element in the C33 gene represents the young AluY family. As expected, BC200 RNA is classified into the oldest fossil AluJo family.

In vitro-synthesized, ^{35}S-labeled murine and human SRP14 were complemented with recombinant SRP9 and incubated with the *in vitro* synthesized biotinylated RNAs. The bound and free proteins were separated using streptavidin beads and the bound protein samples were displayed by SDS–PAGE (Fig. 1). The results demonstrated that all RNAs that are phylogenetically derived from the 7SL RNA gene, except 4.5S RNA, bound human and murine SRP9/14 as well as the two positive controls, 7SL and the Alu-portion of 7SL RNAs (7S-Alu; 36). No specific RNA-binding activity was observed for SRP14 proteins alone (results not shown). These control experiments confirmed that Alu-like RNAs bind exclusively to the heterodimer as previously shown for 7S-Alu and scAlu/LDL RNAs (6). Thus, various scAlu RNAs of different evolutionary ages, including the neuron-specific BC200 RNA, preserved the capacity to bind human and murine SRP9/14. The right as well as the left Alu monomers bound to SRP9/14 suggesting that the dimeric Alu RNA binds two protein subunits. Binding of BC200 RNA to canine SRP9/14 has also been observed (D. Zopf and J. Brosius, personal communications). BC1 RNA, the functional homologue of BC200 RNA which is phylogenetically derived from the tRNA^{Ala} gene, and 4.5S RNA failed to bind SRP9/14. The negative result for 4.5S RNA is most likely explained by changes in the secondary structure of 4.5S RNA as compared with 7SL RNA (31). Finally, two negative controls, U4 RNA and the S portion of 7SL RNA (7S-S), gave the expected negative results.

Production and purification of recombinant mouse and human heterodimers SRP9/14

Having established qualitatively that indeed a large variety of Alu-related RNAs bind to both heterodimers *in vitro*, we wanted

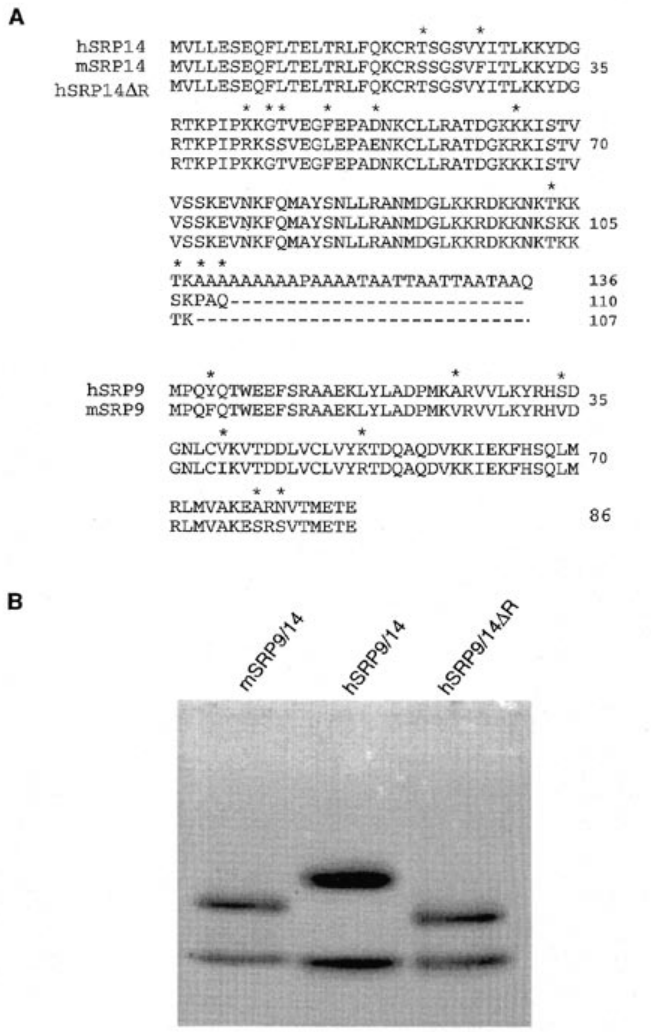

Figure 2. Human and murine SRP9/14 heterodimers. (**A**) Amino acid sequences of the human and murine SRP9 and SRP14 proteins used in the experiments. SRP14ΔR represents the human SRP14 protein with a stop codon at the position 108 in the human protein. (**B**) Coomassie-stained denaturing protein gel of the purified recombinant heterodimers SRP9/14. Lane 1, mouse SRP9/14; lane 2, human SRP9/14; lane 3, human SRP9/14ΔR.

to compare the RNA-binding activities of the proteins in a quantitative way. The three heterodimers analyzed were murine and human SRP9/14 as well as a modified human heterodimer composed of hSRP9 and hSRP14 lacking the additional C-terminal domain (hSRP14ΔR) present in SRP14 proteins of anthropoid species. The comparison between human SRP9/14 and SRP9/14ΔR may reveal a putative role of the C-terminal domain in the activities of the heterodimer, such as RNA-binding and conferring elongation arrest activity to SRP. The primary sequences of the different proteins are compared in Figure 2A. The SRP9 proteins and the common regions of the SRP14 proteins share 92 and 89% identity, respectively.

We used the T7 polymerase-controlled expression system (34) to overproduce the proteins in bacteria. The human proteins, hSRP9, hSRP14 and hSRP14ΔR, were expressed individually in *Escherichia coli*. For the purification of the heterodimer, we combined the crude cell lysates and incubated them for 30 min at

4°C to allow formation of the heterodimer. We always used an excess of SRP9 over SRP14 in the dimerization reactions, since we can easily remove free SRP9 from the heterodimer during purification (Materials and Methods). If synthesized alone, murine SRP14 is rapidly degraded in bacteria (3). To overcome this problem, we produced mSRP9 and mSRP14 from the same plasmid. The expression levels of the proteins were examined by SDS–PAGE (results not shown). Probably because of the difference in stability, murine SRP9 is overproduced compared with SRP14. Thus, mSRP9 is present in excess over mSRP14 during dimer formation in bacteria (Materials and Methods).

The three heterodimers were purified by heparin and CM chromatography. Typically, the proteins were at least 90–95% pure after purification (Fig. 2B) and migrated in SDS–PAGE as expected from their apparent molecular weights. We assumed an equal ratio of both subunits in the purified heterodimers because the excess of SRP9 is removed during the purification procedure. Furthermore, no excess of SRP9 or SRP14 was observed after separation of free and RNA-bound proteins on a glycerol gradient (results not shown).

Recombinant SRP9/14 proteins are biologically active and the additional C-terminal domain in human SRP14 does not affect the activity of the human protein

In order to compare quantitatively the stability of the different RNA–protein complexes, we decided to determine apparent dissociation constants with filter binding experiments. Filter binding experiments have previously been used successfully for determining binding of SRP9/14 to different SRP RNAs (36), and by others to determine binding constants for various RNA–protein complexes (41–43). In the first series of experiments, we determined the apparent dissociation constants of the complexes formed between the heterodimers mSRP9/14, hSRP9/14, hSRP9/14ΔR and the Alu portion of 7SL RNA (7S-Alu).

The ^{32}P-labeled 7S-Alu RNA was synthesized *in vitro* and purified by denaturing gel electrophoresis. The gel-extracted RNA migrated as a single band at the position expected for its size in a denaturing polyacrylamide gel (result not shown). In the simple binding experiments, a constant, very low concentration of ^{32}P-labeled 7S-Alu RNA was titrated against increasing concentrations of the different proteins. RNA–protein complexes were allowed to form in a buffer containing 250 mM potassium acetate and a 50-fold excess in weight of poly(rG) over 7S-Alu RNA. The binding reactions were filtered without dilution and the amount of complex bound to the nitrocellulose filter was determined for each sample by measuring the ^{32}P-labeled 7S-Alu RNA retained on the filter. The negative control, bovine serum albumin instead of the heterodimer, was subtracted from the values obtained in the experiment (Materials and Methods).

The data was analyzed using the Scatchard equation (Materials and Methods) which represents the variables of simple binding experiments in a linear dependence. Three data sets were obtained for each heterodimer and they were fitted by linear regression analysis and normalized to maximal RNA-binding at saturation. The data sets of all three heterodimers fit well to the regression line (Fig. 3A, B and C) and the apparent dissociation constants (app$K_{d'}$) for hSRP9/14, mSRP9/14 and SRP9/14ΔR were calculated from the slope to be 0.191, 1.98 and 0.192 nM, respectively. In the Scatchard equation, complex formation was assumed to be a bimolecular reaction based on a 1:1 ratio of the complex as determined in previous experiments (35) and a possible influence of heterodimer dissociation on RNA–protein complex formation was disregarded. Both assumptions were validated by the experimental findings which showed a linear dependence of all data sets in the concentration range of proteins used in these experiments.

The apparent dissociation constants calculated above needed to be corrected for the different activities of the proteins used in the binding experiments. To this end, we measured complex formation at RNA concentrations 12–100-fold above the dissociation constants determined before. Under these conditions, complex formation is linearly dependent on the protein concentration in the binding reaction and reaches a plateau when the active RNA becomes limiting (Fig. 3D). From the linear dependence of the data at non-saturating protein concentrations, a regression line was derived and from its slope the active fraction of each heterodimer was determined. The activities of the heterodimers hSRP9/14, mSRP9/14 and hSRP9/14ΔR were calculated to be 43, 12 and 45%, respectively. The differences in the activities of the heterodimers may reflect inaccuracies in determining protein concentrations and/or differences in the retention efficiencies of RNA–protein complexes on nitrocellulose filters. The dissociation constants were then corrected taking into consideration the activities of the heterodimers and were calculated to be 0.082, 0.24 and 0.086 nM for hSRP9/14, mSRP9/14 and hSRP9/14ΔR, respectively (Table 1) revealing a remarkable stability of these complexes. These results are also consistent with a previous analysis which concluded that the dissociation constant of synthetic 7SL RNA and canine SRP9/14 is <0.1 nM (46). Furthermore, the very similar appK_d determined for hSRP9/14 and hSRP9/14ΔR indicated that the additional C-terminal domain of hSRP14 has no effect on the RNA-binding characteristic of the human heterodimer. The 3-fold higher dissociation constant of the murine heterodimer could be explained by an intrinsic difference in the RNA-binding capacities of the two proteins and/or by differences between the Alu portions of murine and synthetic 7SL RNA. The sequence of the murine 7SL RNA is only partially known to date (47).

We have previously shown that murine SRP9/14 can functionally replace canine SRP9/14 in conferring elongation arrest activity to the particle (35). Similar experiments with the human SRP9/14 proteins demonstrated that they have the same capacity to confer elongation arrest activity to the particle as their murine counterpart (results not shown). These results further confirmed the biological activity of the human proteins.

Human and murine SRP9/14 have significantly different affinities for Alu-like RNAs

To quantify the affinities of the three heterodimers, hSRP9/14, mSRP9/14 and hSRP9/14ΔR, for the different Alu-like RNAs, which we found to bind the proteins in the initial experiments, we performed direct competition experiments. Increasing amounts of competitor RNAs were incubated with constant amounts of ^{32}P-labeled 7S-Alu RNA and of protein. All competitor RNAs used in the experiments were synthesized *in vitro* by T7 RNA polymerase and purified by denaturing gel electrophoresis. The gel-extracted RNAs migrated as single RNA species at the positions expected for their sizes (results not shown). Based on the results obtained in the simple binding experiments, the amount of protein used in these experiments was chosen to ensure at least 98% binding of the protein to the RNA. To test the assay,

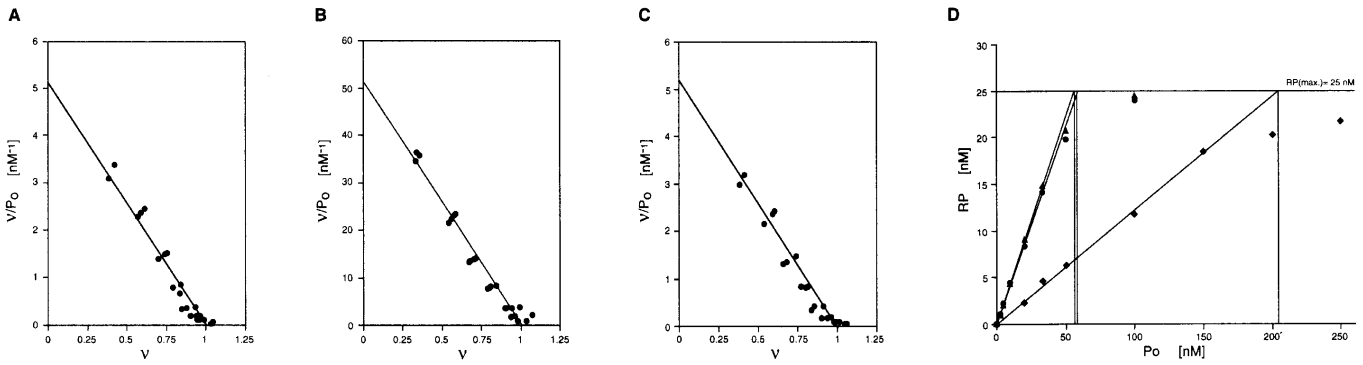

Figure 3. Determination of dissociation constants for 7S-Alu RNA and different heterodimers using Scatchard analysis. (**A**) Human SRP9/14; (**B**) mouse SRP9/14, (**C**) human SRP9/14ΔR. P_0 represents the protein concentration [nM] in the binding experiments; υ represents the fraction of RNA in the complex at the protein concentration P_0. The fraction of RNA in the complex at saturating protein concentrations was normalized to 1. hSRP9/14$K_{d'}$ = 0.191 nM; mSRP9/14 $K_{d'}$ = 1.98 nM; hSRP9/14ΔR $K_{d'}$ = 0.192 nM. (**D**) Stoichiometric complex formation at RNA and protein concentrations above the dissociation constants determined in A, B and C. RP: RNA–protein complex. The activities of the proteins were determined from the initial slopes of the straight lines to be 43, 12 and 45% for hSRP9/14, mSRP9/14 and hSRP9/14ΔR, respectively.

Table 1. Dissociation constants for human and mouse SRP9/14–RNA complexes

	Human SRP9/14			Mouse SRP9/14				Human SRP9/14ΔR		
RNA	$\frac{K_{dcomp}}{K_{d7S-Alu.}}$	Kd [nM]	ΔG°'	$\frac{K_{dcomp}}{K_{d7S-Alu.}}$	Kd [nM]	ΔG°'	$\frac{K_{dm}}{K_{dh.}}$	$\frac{K_{dcomp}}{K_{d7S-Alu.}}$	Kd [nM]	ΔG°'
7S-Alu	1.0	0.082±0.01	-12.74	1.0	0.24 ±0.03	-12.15	2.9	1.0	0.086±0.01	-12.71
BC200	1.5	0.12 ±0.01	-12.53	4.2	1.01 ±0.01	-11.36	8.2	1.5	0.13 ±0.01	-12.49
scAlu/α-feto	2.0	0.16 ±0.01	-12.37	13.0	3.12 ±0.1	-10.74	19.0	1.9	0.17 ±0.02	-12.34
scAlu/LDL	3.3	0.27 ±0.01	-12.09	73.0	17.5 ±1.6	-9.8	54.4	3.5	0.3 ±0.01	-12.03
scB1	15.0	1.23 ±0.05	-11.25	33.5	8.04 ±0.2	-10.22	6.5			
Right	17.3	1.42 ±0.04	-11.18							

The RNAs are described in the text. The free energy of complex formation (ΔG°′) is indicated in kcal/mol.

we first used 7S-Alu RNA as a competitor in the binding experiments with the three heterodimers. The average of two data sets collected for each heterodimer was analyzed according to equation **3** which represents the variables of the competition experiments in a linear dependence (Materials and Methods). Linear regression was used to fit the data (Fig. 4A, B and C, line 1). The close fit of the data to a straight line through the origin confirmed the basic assumption for the mathematical model including again the 1:1 stoichiometry of RNA and SRP9/14 in the complex. From the slope of the line, the relative ratios of the apparent dissociation constants of the competitors (app$K_d$comp) and of 7SL RNA (appK_d7S-Alu) can be calculated. With 7S-Alu as a competitor, the ratio was found to be 1.0 confirming that the experimental conditions matched the mathematical model. The negative control, U2 snRNA, was shown to compete only at very high concentrations of competitor RNA with an appK_d at least 500-fold higher than that of 7S-Alu (results not shown). The Alu-like RNAs which were found to bind SRP9/14 in the initial experiments were then used as competitors in the binding experiments and the appK_d was determined as before. The values of the data sets were found to fit well to a straight line for all RNAs analyzed (Fig. 4A, B and C). The relative ratios of the apparent dissociation constants and their calculated absolute values are shown in Table 1. The relative and absolute dissociation constants between the two human heterodimers were almost identical for all four RNAs analyzed. These results demonstrated clearly that the C-terminal part of hSRP14 is not involved in the RNA-binding function of human SRP9/14. We therefore decided to drop competition experiments with scB1 and the right Alu monomer RNAs. The dissociation constants of the human heterodimer and the different Alu-like RNAs increase in parallel to the evolutionary distance between the tested RNAs and 7SL RNA. The murine scB1 RNA and the right Alu monomer RNA have the lowest, however still rather high, affinities for the protein. The relative apparent dissociation constants for the murine RNA–protein complexes increase much more rapidly than for the human RNA–protein complexes. Thus, the relative as well as the absolute dissociation constants for murine SRP9/14 and scB1 RNA are higher than the corresponding values for human SRP9/14. The relative affinities of the murine protein for scAlu/LDL and scB1 RNAs are reversed as compared with the human protein. Similar dissociation constants for 7SL, scAlu and scB1 RNAs and the human SRP9/14 protein have previously been determined using a mobility shift assay (29). They are a factor of 1.5 to 3 higher than the dissociation constants determined here. However, the activity of the protein in complex formation was not determined in the mobility shift assays which might explain the observed difference.

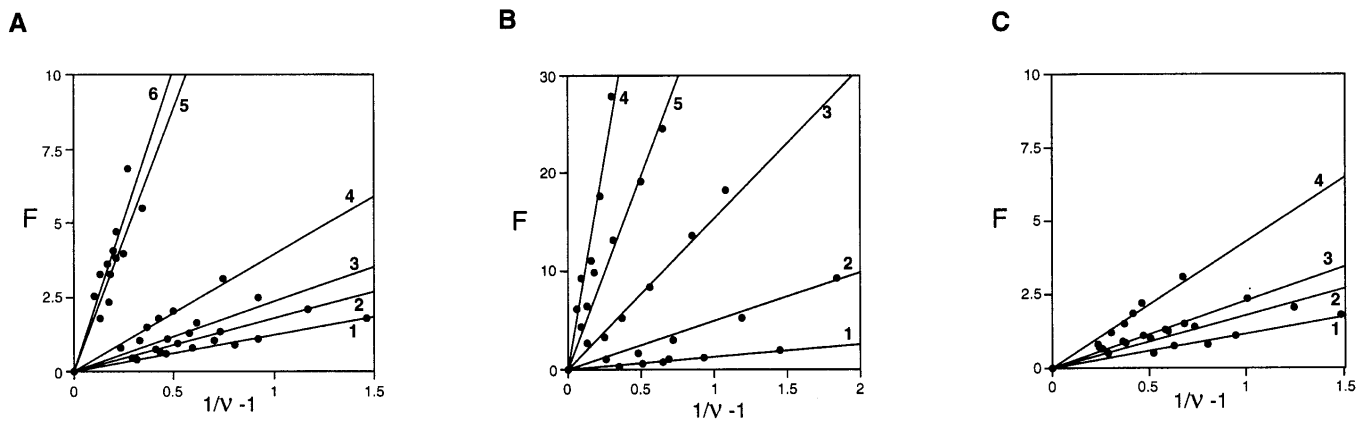

Figure 4. Dissociation constants of RNA–protein complexes formed between various Alu-like RNAs and different heterodimeric proteins determined by competition experiments. (**A**) Human SRP9/14, (**B**) mouse SRP9/14, (**C**) human SRP9/14ΔR. The competitor RNAs used were as follows: **1**, 7S-Alu; **2**, BC200; **3**, scAlu/α-feto; **4**, scAlu/LDL; **5**,υ scB1; and **6**, right Alu monomer. υ represents the fraction of 7S-Alu RNA in the complex at the competitor concentration R_0comp. υ represents the fraction of RNA in the complex in the absence of competitor.

DISCUSSION

We have shown that the SRP subunit, SRP9/14, can bind with high affinity to a large range of Alu-like RNAs of different evolutionary ages and of primate and rodent origin, including the neuron-specific primate BC200 RNA. Dissociation constants within and below the nanomolar range, as we observed for all complexes, are quite low as compared with dissociation constants of other RNA–protein complexes (41,43,48), revealing highly specific interactions between the RNAs and the proteins. Furthermore, the high affinities of the complexes make it very likely that SRP9/14 is indeed associated with all Alu-like RNAs *in vivo* as has been demonstrated for scAlu RNAs (6). This interpretation is further supported by the finding that dimeric Alu and BC200 RNAs exist as RNPs *in vivo* (6,23; Jr-G. Cheng, H. Tiedge and J. Brosius, personal communication).

Although all Alu-like RNAs bind very efficiently to human SRP9/14, there is a defined hierarchy in the binding affinities of the different Alu-related RNAs that parallels the evolutionary distance between the Alu RNA and the 7SL RNA genes. In general, more efficient binding occurs with RNAs that are derived from the FLAM element. The BC200 RNA represents the closest relative of 7SL RNA followed by the scAlu/α-feto (AluS subfamily) and scAlu/LDL RNAs (AluYb8 subfamily). The rodent specific scB1 RNA and an RNA derived from a right Alu monomer, which is related to the primitive FRAM gene and belongs to the young AluY family, have the lowest affinity for human SRP9/14. By comparing the affinities of human and mouse SRP9/14 for various Alu-like RNAs, we found that the absolute and relative affinities of the human protein for all RNAs are higher than those of the murine protein. These results suggest that the RNA-binding capacity of human SRP9/14 may have improved to ensure efficient binding of the protein even to distantly related Alu RNAs, like RNAs derived from recently transposed Alu family members. Although the absolute affinity of scB1 RNA for mouse SRP9/14 is lower than for human SRP9/14, the difference between them is the lowest for all RNAs analyzed except 7S-Alu RNA (Table 1) indicating that cytoplasmic scB1 RNAs were selected to preserve a minimal affinity for the murine heterodimer.

The differences in RNA-binding affinities observed between the human and the murine heterodimer are not explained by the additional C-terminal domain in the anthropoid SRP14 protein, since the removal of this domain has no effect on RNA-binding. This result is consistent with the previous observation that C-terminal domains in SRP9 and SRP14 are not involved in 7SL RNA-binding (35). The difference in free energy of complex formation is smallest for 7S-Alu RNA (0.6 kcal/mol) and most significant for scAlu/LDL RNA (2.3 kcal/mol) and may be explained by relatively subtle differences in the molecular interactions in the complex, such as the loss of one or two hydrogen bonds. There are indeed only a few changes in the primary sequences between the SRP14 and SRP9 polypeptides (Fig. 2). In SRP9 and SRP14, two and four of the amino acid changes, respectively, are located in C-terminal regions which have been shown to be dispensable for 7SL RNA-binding (35). In SRP9, the five other differences in amino acid sequence are spread over the whole polypeptide whereas in SRP14, five of the remaining eight amino acid changes cluster into a region of the protein which we found to be implicated in 7SL RNA-binding (N. Bui and K.S., unpublished results). This suggests that changes in this domain may play a role in conferring differential RNA-binding capacities to the mouse and human heterodimers.

The diversity as well as the stability of these complexes strongly suggest cellular functions for Alu-like scRNPs which may be different for individual particles. For BC200 RNP, such a function is also indicated by the regulated expression of its RNA subunit from a single gene in certain neuron cells and by its very specific location to the somato-dentritic region in these cells (24,25). The striking structural resemblance of the protein and RNA subunits of Alu-like scRNPs and the Alu-domain of SRP strongly suggests a similarity in function. Thus, functions of BC200 RNP may be related to translation and/or to targeting of nascent chains to the somato-dentritic region. Interestingly, the putative functional homologue of BC200 RNA in rodent cells, the BC1 RNA, is derived from a tRNA gene (49–51). The progenitors for both RNAs are intimately involved in the translation process, thus, further supporting a putative function for these RNPs in association with the ribosome.

BC1 RNA does not bind to SRP9/14. Thus, other RNAs that are phylogenetically related to tRNAs, such as B2 RNA in rodent cells, might not bind SRP9/14. Cytoplasmic B2 RNAs in rodent cells are more abundant than scB1 RNAs (14,52,53). In analogy to the neuron-specific RNPs described above, it is conceivable that putative functions of scAlu and Alu RNPs in human cells may be accomplished by scB1 and B2 RNPs in rodent cells. This possibility could, at least partially, explain the apparent lower constraint on the murine protein to preserve efficient binding to Alu-like RNAs.

The anthropoid specific excess of SRP9/14 may have been required to compensate a defect in SRP assembly and/or functions. Our experiments failed to reveal a defect in RNA-binding and in conferring elongation arrest activity to the particle. This together with an increased affinity of human SRP9/14 for distantly related Alu RNAs, such as recently transposed elements, may indicate that the anthropoid specific excess of SRP9/14 is related to Alu amplification rather than to SRP activity. A role for the excess of SRP9/14 in repressing Alu retroposition has been hypothesized based on the observation that the appearance of an excess of SRP9/14 coincides with a dramatic reduction in amplification of Alu sequences in early anthropoid evolution (8). Gene duplication and the acquisition of an additional domain in one of the SRP14 genes may have fortuitously changed the expression level of SRP14 which in turn caused an increase in SRP9 expression. According to the hypothesis, the binding of Alu RNAs to the excess of SRP9/14 may have removed the transcript from the retroposition pathway thereby repressing Alu amplification. The preserved high affinity of human SRP9/14 for younger Alu RNAs is consistent with the hypothesized repressive role of SRP9/14 in Alu amplification. Only very young Alu elements have been found to retrotranspose recently (54), possibly, because their lower relative affinity for SRP9/14 may have increased their chances to escape SRP9/14 repression.

ACKNOWLEDGEMENTS

We thank Drs J. Brosius, P. Fabrizio, W. R. Jelinek, A. Krämer, H. Leffers, R. Maraia, O. Yoshie and D. Zopf for the plasmids used in these studies. We are also grateful to Drs J. Brosius and D. Zopf for communicating unpublished results and to O. Weichenrieder for help in initial calculations. We thank Monique Fornallaz for her technical assistance. This work was supported by a grant from the Swiss National Science Foundation and the Canton de Genève. K.S. is a fellow of the START program of the Swiss National Science Foundation.

REFERENCES

1 Walter, P. and Johnson, A. E. (1994) *Annu. Rev. Cell Biol.*, **10**, 87–119.
2 Lütcke, H. (1995) *Eur. J. Biochem.*, **228**, 531–550.
3 Strub, K., Wolff, N. and Oertle, S. (1993) In Nierhaus, K. H., Franceschi, F., Subramanian, A. R., Erdmann, V. A. and Wittmann-Liebold, B. (eds) *The Translational Apparatus*. Plenum Press, New York, pp. 635–645.
4 Siegel, V. and Walter, P. (1986) *Nature*, **320**, 81–84.
5 Strub, K. and Walter, P. (1990) *Mol. Cell. Biol.*, **10**, 777–784.
6 Bovia, F., Fornallaz, M., Leffers, H. and Strub, K. (1995) *Mol. Biol. Cell*, **6**, 471–484.
7 Chang, D.-Y., Nelson, B., Bilyeu, T., Hsu, K., Darlington, G. and Maraia, R. J. (1994) *Mol. Cell. Biol.*, **14**, 3949–3959.
8 Chang, D. Y., Sasaki Tozawa, N., Green, L. K. and Maraia, R. J. (1995) *Mol. Cell Biol.*, **15**, 2109–2116.
9 Chang, D. Y. and Maraia, R. J. (1993) *J. Biol. Chem.*, **268**, 6423–6428.
10 Bovia, F. and Strub, K. (1996) *J. Cell Sci.*, **109**, 2601–2608.
11 Matera, A. G., Hellmann, U. and Schmid, C. W. (1990) *Mol. Cell. Biol.*, **10**, 5425–5432.
12 Maraia, R. J., Driscoll, C. T., Bilyeu, T., Hsu, K. and Darlington, G. J. (1993) *Mol. Cell Biol.*, **13**, 4233–4241.
13 Schmid, C. W. and Shen, C.-K. J. (1985) In MacIntyre, R. J. (ed.) *Molecular Evolutionary Genetics*. Plenum Publishing Corp., New York, Vol. pp. 323–358.
14 Weiner, A. M., Deininger, P. L. and Efstratiadis, A. (1986) *Annu. Rev. Biochem.*, **55**, 631–661.
15 Britten, R. J. (1994) *Proc. Natl. Acad. Sci. USA*, **91**, 6148–6150.
16 Deininger, P. L. and Daniels, G. R. (1986) *Trends Genet.*, **2**, 76–80.
17 Daniels, G. R., Fox, G. M., Loewensteiner, D., Schmid, C. W. and Deininger, P. L. (1983) *Nucleic Acids Res.*, **11**, 7579–7593.
18 Shen, M. R., Batzer, M. A. and Deininger, P. L. (1991) *J. Mol. Evol.*, **33**, 311–320.
19 Jurka, J. and Zuckerkandl, E. (1991) *J. Mol. Evol.*, **33**, 49–56.
20 Quentin, Y. (1992) *Nucleic Acids Res.*, **20**, 3397–3401.
21 Quentin, Y. (1992) *Nucleic Acids Res.*, **20**, 487–493.
22 Kapitonov, V. and Jurka, J. (1996) *J. Mol. Evol.*, **42**, 59–65.
23 Liu, W. M., Maraia, R. J., Rubin, C. M. and Schmid, C. W. (1994) *Nucleic Acids Res.*, **22**, 1087–1095.
24 Martignetti, J. A. and Brosius, J. (1993) *Proc. Natl. Acad. Sci. USA*, **90**, 11563–11567.
25 Tiedge, H., Chen, W. and Brosius, J. (1993) *J. Neurosci.*, **13**, 2382–2390.
26 Quentin, Y. (1994) *Nucleic Acids Res.*, **22**, 2222–2227.
27 Adeniyi-Jones, S. and Zasloff, M. (1985) *Nature*, **317**, 81–84.
28 Maraia, R. J. (1991) *Nucleic Acids Res.*, **19**, 5695–5702.
29 Hsu, K., Chang, D. Y. and Maraia, R. J. (1995) *J. Biol. Chem.*, **270**, 10179–10186.
30 Jelinek, W. R. and Schmid, C. W. (1982) *Annu. Rev. Biochem.*, **51**, 813–844.
31 Labuda, D. and Zicetkiewicz, E. (1994) *J. Mol. Evol.*, **39**, 506–518.
32 Bui, N., Bovia, F., Wolff, N., Morrical, M. D., Walter, P. and Strub, K. (unpublished results) X78305.
33 Strub, K. and Walter, P. (1989) *Proc. Natl. Acad. Sci. USA*, **86**, 9747–9751.
34 Studier, F. W., Rosenberg, A. H., Dunn, J. J. and Dubendorff, J. W. (1990) *Methods Enzymol.*, **185**, 60–89.
35 Bovia, F., Bui, N. and Strub, K. (1994) *Nucleic Acids Res.*, **22**, 2028–2035.
36 Strub, K., Moss, J. and Walter, P. (1991) *Mol. Cell. Biol.*, **11**, 3949–3959.
37 Gibbs, P. E. M., Zielinski, R., Boyd, C. and Dugaiczyk, A. (1987) *Biochem.*, **26**, 1332–1343.
38 Schoeniger, L. O. and Jelinek, W. R. (1986) *Mol. Cell. Biol.*, **6**, 1508–1519.
39 Imai, T., Fukudome, K., Takagi, S., Nagira, M., Furuse, M., Fukuhara, N., Nishimura, M., Hinuma, Y. and Yoshie, O. (1992) *J. Immunol.*, **149**, 2879–2886.
40 Scatchard, G., Coleman, V. S. and Shen, A. L. (1957) *J. Am. Chem. Soc.*, **79**, 12–20.
41 Carey, J. and Uhlenbeck, O., C. (1983) *Biochemistry*, **22**, 2610–2615.
42 Hall, K. B. and Kranz, J. K. (1995) *Methods Enzymol.*, **259**, 261–281.
43 Romaniuk, P. J. (1985) *Nucleic Acids Res.*, **13**, 5369–87.
44 Martignetti, J. A. and Brosius, J. (1995) *Mol. Cell. Biol.*, **15**, 1642–1650.
45 Jurka, J. and Milosavljevic, A. (1991) *J. Mol. Evol.*, **32**, 105–121.
46 Janiak, F., Walter, P. and Johnson, A. E. (1992) *Biochemistry*, **31**, 5830–5840.
47 Balmain, A., Krumlauf, R., Vass, J. K. and Birnie, G. D. (1982) *Nucleic Acids Res.*, **14**, 4259–4277.
48 Hall, K., B. and Kranz, J., K. (1995) *Methods Enzymol.*, **259**, 261–281.
49 Dechiara, T. M. and Brosius, J. (1987) *Proc. Natl. Acd. Sci. USA*, **84**, 2624–2628.
50 Tiedge, H., Fremeau, R. T., JR., Weinstock, P. H., Arancio, O. and J., B. (1991) *Proc. Natl. Acad. Sci. USA*, **88**, 2093–2097.
51 Kim, J., Martignetti, J. A., Shen, M. R., Brosius, J. and Deininger, P. (1994) *Proc. Natl. Acad. Sci. USA*, **91**, 3607–3611.
52 Ryskov, A. P., Ivanov, P. L., Kramerov, D. A. and Georgiev, G. P. (1983) *Nucleic Acids Res.*, **11**, 6541–6558.
53 Kramerov, D. A., Lekakh, I. V., Samarina, O. P. and Ryskov, A. P. (1982) *Nucleic Acids Res.*, **10**, 7477–7491.
54 Shaikh, T. H. and Deininger, P. L. (1996) *J. Mol. Evol.*, **42**, 15–21.